NEW METHOD OF INTERFACIAL AND MICRO-DAMAGE SENSING OF COMPOSITES VIA PENCIL LEAD DRAWING PAPER SENSOR (PLDPS) AND ELECTRICAL RESISTANCE (ER) MAPPING

Joung-Man Park[1,2†], Ha-Seung Park[1], Pyeong-Su Shin[1], Jong-Hyun Kim[1], Yeong-Min Baek[1], Lawrence K. DeVries[2]

[1]Department of Materials Engineering and Convergence Technology, Center for Creative Human Resource & Convergence Materials, Research Institute for Green Energy Convergence Technology, Gyeongsang National University, Jinju 52828, Republic of Korea

[2]Department of Mechanical Engineering, The University of Utah,

Salt Lake City, Utah 84112, U.S.A.

ABSTRACT

The pencil drawing paper sensor (PLDPS) is a flexible and wearable sensing device. A new concept sensor offers tremendous potential feasibility for a variety of applications. It is highly responsive, sensitive, low cost, easily handles pencil lead-graphite on paper and can be made from cellulose pulp fibers extracted from wood, rags or grass, which are inexpensive, nature-friendly materials. Sensing effects, on 3 different papers (Plane, Hwasun, and Han papers) based on the properties of PLDPS, were compared using FT-IR, tensile tests, optical observations and electrical resistance (ER). Interfacial and mechanical properties of epoxy and GF/epoxy composites were evaluated by damage sensing and ER mapping using PLDPS during impact, flexural, and interlaminar shear strength (ILSS) testing. Plane paper was found to the optimal type of paper for use as the adherend for the pencil sensor. Glass fiber (GF)/epoxy composites were severely damaged, and as a result large ER changes of the PLDPS were observed.

1. INTRODUCTION

A sensor might be described as a material that can detect external stress or external environment by an electrical signal [1]. The conductive material of the sensor may, in some cases, be a small-sized sensor in an optimal form having moisture, temperature, or a specific gas sensing ability [2]. Carbon is an important electric conductor material because of its varying structural and morphological forms [3]. These forms include: graphite and diamond allotropes (highly oriented pyrolytic graphite, glassy carbon, carbon fiber electrodes, boron-doped diamond electrode) [4], carbon particles mixed with a suitable binder (carbon paste and carbon composite electrodes) [5], carbon nanomaterials (carbon nanotubes, graphene) [6] which may be useful electrodes or sensors and are used as conductors in areas where conductivity is required. Among these, the graphite of

Copyright 2019. Used by the Society of the Advancement of Material and Process Engineering with permission.

SAMPE Conference Proceedings. Charlotte, NC, May 20-23, 2019. Society for the Advancement of Material and Process Engineering – North America.

pencil is used for more purposes in comparison with other carbon-based materials such as glassy carbon, carbon paste and diamond [7]. This is because pencil graphite is highly reactive, sensitive, low cost, and easy to handle [8] compared to other materials. Paper is a thin material made from cellulose, pulp fibers extracted from wood, rags or grass and then dried into a flexible sheet, making it an inexpensive natural material [9]. Paper provides an ideal coarse surface where black pencil marks are created by mechanical abrasion of graphite particles from a pencil [10]. Pencil lead is primarily composed of graphite, which is a carbon isotope, and aluminosilicate clay with wax used as binder.

This study involves basic research to develop a sensor capable of detecting external stress or external environment by means of electrical signals. In many countries, studied in an effort to find the most optimized paper for use with PLDPS through basic research on the development of sensors for pencil lead with cellulose based paper. The paper suitable for PLDPS was evaluated through tensile test and initial ER according to the kind of paper. The interfacial and mechanical properties of epoxy and GF/epoxy composites were evaluated via damage sensing and mapping using PLDPS with impact, flexural, drilling and ILSS tests.

2. EXPERIMENTATION

2.1 Materials and specimens

The pencil (HB, 2B, 4B, and 6B, Tombow, Japan) was used for the electrode materials and plain paper (A4, Double A, Thailand), Han paper (Gogamhanji, Korea) were used as a substrate. A pencil was drawn on paper with a constant force using a load cell. The copper wire and PLDPS were bonded with silver paste and fixed with epoxy adhesive (Huntsman, USA). The bisphenol A-type epoxy (YD-128) and amine type curing agent (D-400, D-2000) (Kukdo Chemical Co, Korea) were used as the matrix and adhesives to attach and PLDPS to the specimen. YD-128 and D-400 were mixed at a ratio of 10: 6 and used as a matrix. YD-128, D-400 and D-2000 were mixed at a ratio of 10: 5.4: 0.6 and used as an adhesive. The matrix and adhesive were cured with a drying oven (FO-600M, Jeio tech, Korea) at 80 ºC for 2 hours and then 120 ºC for 2 hours. The ER was measured using a multimeter (34401A, Jillian Tech, USA).

Figure 1(a) shows the schematic for measuring the load on the paper using a pencil, and measure the actual load. A pencil lead was used to draw PLDPS with a force of 0.8 kg_f on paper. When a force more than 0.8 kg_f was applied, the arrangement of cellulose fibers was disturbed and resulted in decreasing the strength of the PLDPS. When the force was weaker, the pencil lead was not drawn on the paper. Figure 1(b) was a photograph of the surface of the PLDPS using SEM. The FT-IR spectrum of graphite of pencil lead which is displayed in figure 1(c) depicts a strong -OH peak at 3429 cm^{-1}[18] and the sp^2 carbon of C=C shows the stretching vibration peak at 1633 and 1588 cm^{-1} and =C-H vending vibration peak at 1377 cm^{-1}. It also shows the stretching vibration peak due to the antisymmetric and symmetric mode of CH_2 at 2920 and 2846 cm^{-1}.

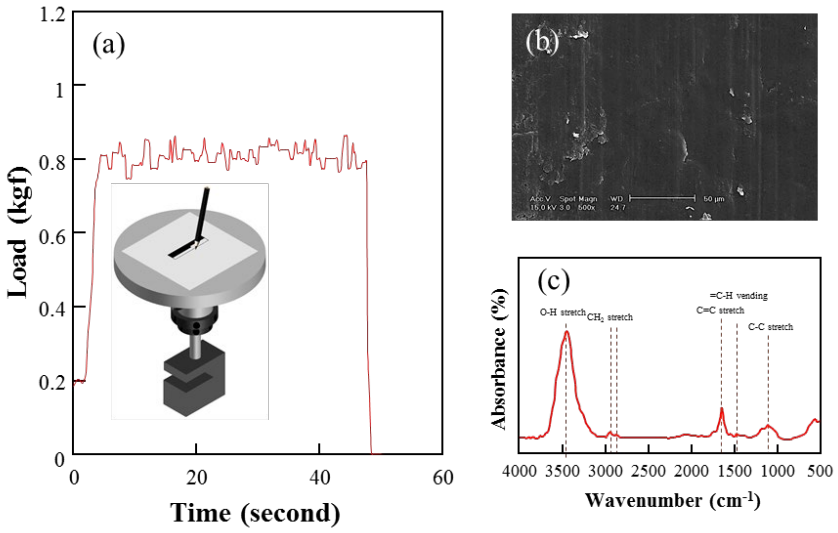


Fig. 1. Schematic plots of the process to manufacture PLDPS: (a) schematic of pencil drawn on the paper to manufacture PLDPS; (b) FE-SEM picture of PLDPS; (c) FT-IR spectrum of pencil lead

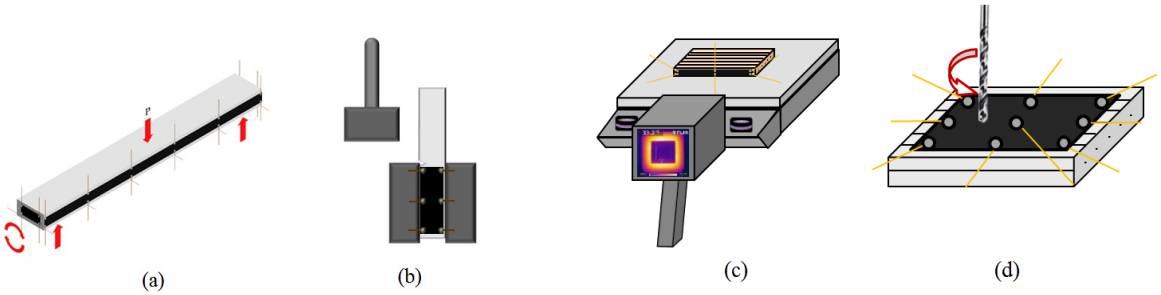


Fig. 2. Schematic plots of various specimens with attaching PLDPS: (a) flexural; (b) Izod; (c) heat; and (d) drilling tests

Figure 2 shows the schematic plots of various typed tests including flexural, Izod, heat and drilling tests. To detect the mechanical damage and heat, each PLDPS was attached upper and ahead on the GFRC specimens like figure 2. Chosen paper coated with pencil lead was installed with cupper wire probes fixed by silver paste and epoxy adhesive.

2.2 Experimental methods

40 tensile specimens were prepared with Plain and Han papers. Tensile tests were performed using a universal testing machine (UTM) (H1K-S, Lloyd, U.K.) on specimen with a gauge length of 20 mm at testing speeds of 0.5 mm/minute. The tensile test results were statistically analyzed using unimodal Weibull distributions. Fiber failure analysis used for the unimodal cumulative Weibull distribution function based on one type defect is

$$F(t) = 1 - \left\{ p\, exp\left[-\left(\frac{t}{\alpha_1}\right)^{\beta_1} \right] q \exp + \left[-\left(\frac{t}{\alpha_2}\right)^{\beta_2} \right] \right\} \quad (1)$$

$$p + q = 1$$

where t is the tensile strength of papers p and q are the portions of the low and high strength population while α_1, β_1 and α_2, β_2 are the scale and shape parameters for the low and high strength portions, respectively.

The tensile, Izod impact and flexural strength tests of epoxy resins were performed by ASTM D638, ASTM D256 and ASTM D790. The impact hammer energy and impact speed were 6.8 J and 3.5 m/s. Ten specimens of each type were tested in all tests. The tensile test was carried out using a universal material testing machine (LR 10K, Lloyds, UK) after preparing specimens with a gauge length of 2 cm and a width of 1 cm. The initial ER was measured using a multimeter (34401A, Jillian Tech, USA). Composite materials were prepared by laminating four unidirectional mats using the Resin Transfer Molding (RTM) method, cured at 80 ºC for 2 hours and 120 ºC for 2 hours at 10 MPa pressure after resin injection. The thermographic images, measured with a thermogram camera (FLIR E40, FLIR system, U.S.A.), were compared with the PLDPS sensibility to heat flow.

3. RESULTS

3.1 Bending tests of PLDPS

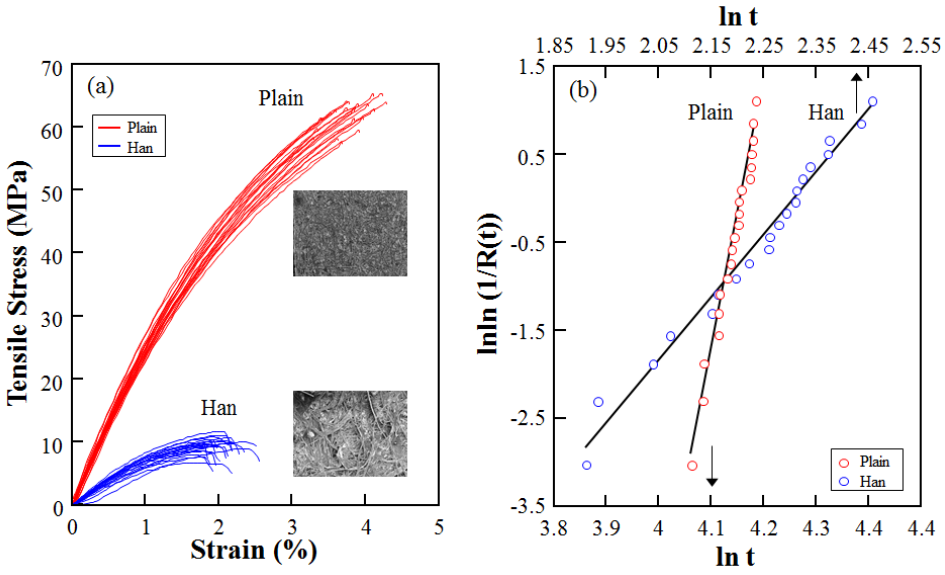


Fig. 3. Tensile test results for A4 and Han paper: (a) S-S curve; and (b) Weibull distribution for the paper tensile strength

Figure 3(a) shows the results of tensile tests using each paper to obtain stress-strain curves. The tensile strength was 39 MPa and the elongation was approximately 4%. The lowest tensile strength and elongation a tensile strength of 10 MPa and an elongation at 2% were the lowest. On the other hand, plain paper has a tensile strength of 63 MPa and an elongation of about 4%, which indicates that the tensile strength was high and that the elongation was also good. Tensile test results show that the damage caused by PLDPS itself was minimal when PLDPS was produced by drawing a pencil line on plain paper. In addition, the Weibull distribution for tensile strength as shown in figure 3(b), which shows that Plain paper and Han paper have a very narrow distribution whereas Han paper has a relatively wide Weibull distribution. As a result, the tensile strength of plain paper was relatively uniform but Han paper was not.

3.2 Bending test of PLDPS

Figure 4(a-b) shows PLDPS fixed at both ends between two glass plates to measure ER changes due to bending. The distances between the two glass plates was gradually narrowed to 2 cm, 1.5 cm, 1 cm, 0.5 cm, and 0 cm, and was gradually moved away from 0 cm to determine the ER change of PLDPS. ER changes increased as the distance decreased whereas it decreased as the distance increased. The ER changed abruptly with the change of the distance, but the ER remained constant for a fixed distance. As the distance between the two glass plates decreased, the distance between the pencil lead particles increased as the PLDPS warped.

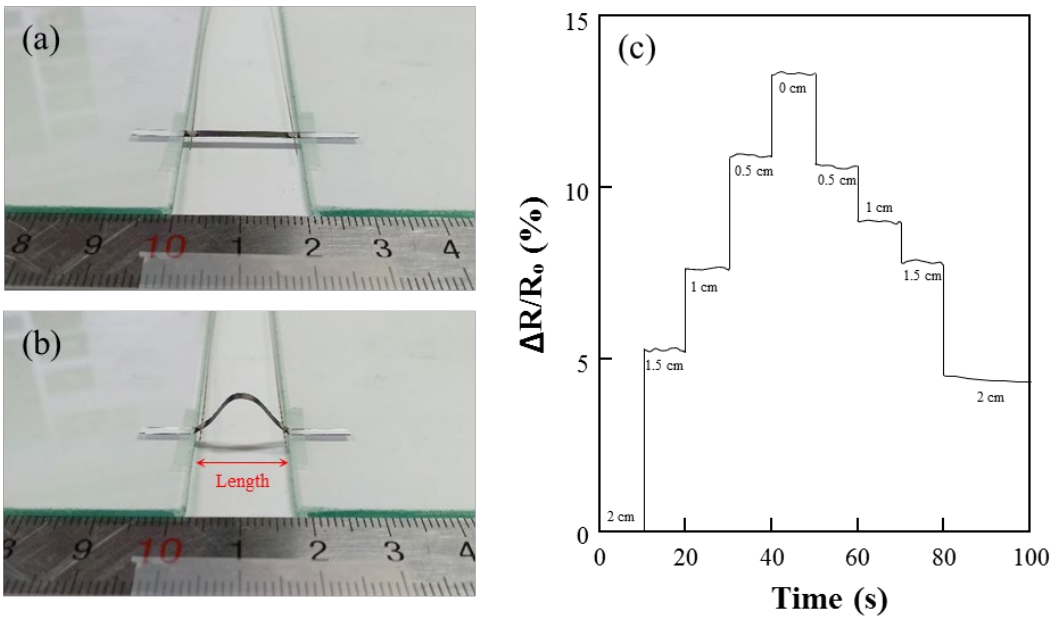


Fig. 4. Measuring the ER change for PLDPS in bending: (a-b) pictures of PLDPS fixed at both ends between two glass plates for measurement of ER change during bending; and (c) the ER change in PLDPS during bending

3.3 AE and ER evaluation of CFRP during aging

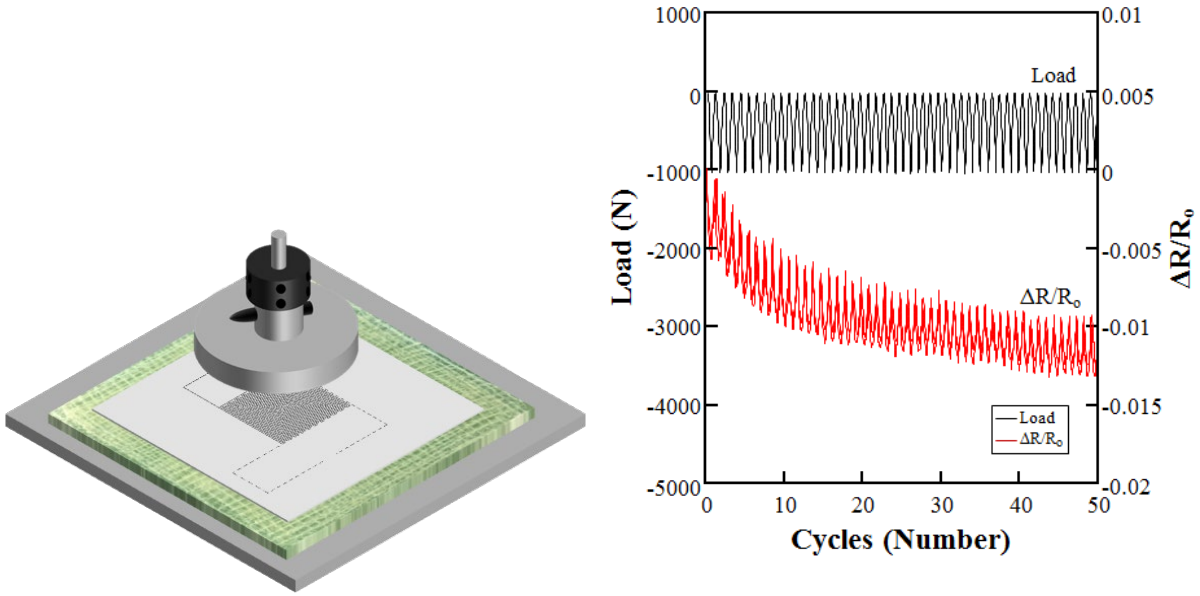


Fig. 5. Measuring ER change of square-spiral PLDPS during cyclic compression testing

Figure 5 shows the results during cyclic compression tests using a plain paper at the bottom of a composite specimen with a rectangular vortex PLDPS. The black line represents the curve of the compressive force during cyclic loading, and the red line represents the change in ER with respect to the initial ER as a percentage. As a result, pencil lead particles are compressed and compacted, thus reducing ER. In the section where the compression force decreases, the pencil lead particles recover to relatively near original volume, and increasing the ER. As this cycle is repeated, the degree of recovery of the compressed pencil lead particles decreases and they become denser, so the overall ER decreases. This means that it is possible to observe the compressive force, which changes during repeated compression test of composite materials, with PLDPS.

3.4 Impact sensing of PLDPS

Figure 6(a) shows results of experiments to evaluate ER change as a function of the notch and PLDPS distances. When the distance between the notch and the PLDPS was 2.5 cm, the change of in ER was 0.002, but it increased more than 0.02 at 0.5 cm. These results lead to inferences that the degree of damage may vary depending on the area of the impact specimen, so the mapping experiment using PLDPS as shown in figure 6(b) was performed. In figure 6(b), the upper left corner of the mapping graph is near the notch, where the damage is much higher than at other areas. PLDPS was restored to its original ER after some time subsequent to its rapid increase due to the impact applied by the hammer of the Izod machine.

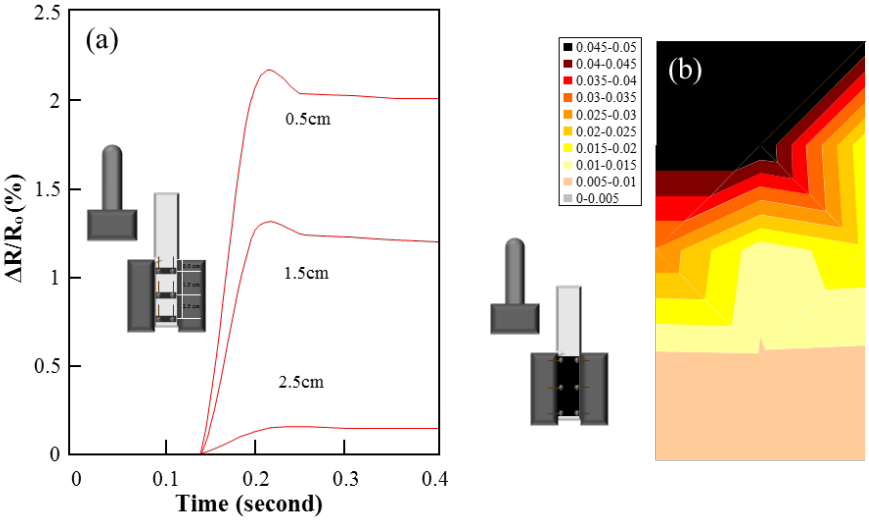


Fig. 6. Measuring ER change of PLDPS during impact testing: (a) comparison of ER change for different distances between notch and PLDPS; and (b) Impact strength detection using PLDPS 2d mapping

3.5 Flexural mapping of PLDPS

Figure 7 shows damage mapping of the PLDPS in flexure testing. It confirms that the ER change was largest in areas where the specimen was most highly deformed. Even a specimen consisting of a single mass had a larger change in ER due to a stronger deformation at the center than at the edge and at the lower surface than at the side. Also, the flexural strain increased to 0.34% compared with 0.17%, and the ER change also increased drastically as the deformation progressed.

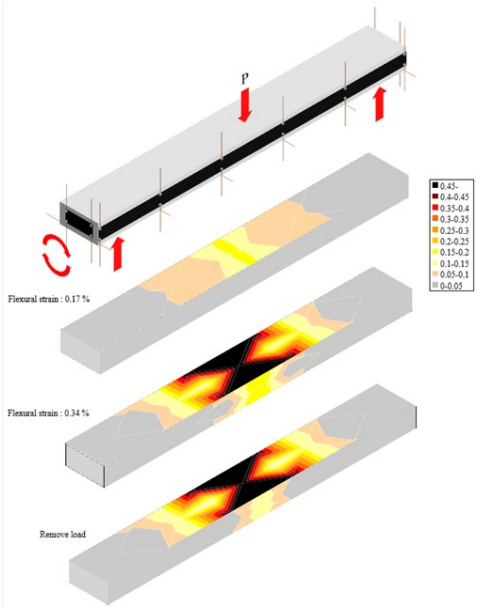


Fig. 7. Measured ER change of PLDPS in a flexural test

3.6 Thermal mapping of PLDPS

Upon heating the PLDPS, the graphite becomes activated and the electrical resistance decreases. To prove the thermal tensing, thermograms were used and figure 8 shows the detected thermal conductivity with time using PLDPS and thermograms. The material was heated from the bottom and the PLDPS sensed as well as the thermogram detected.

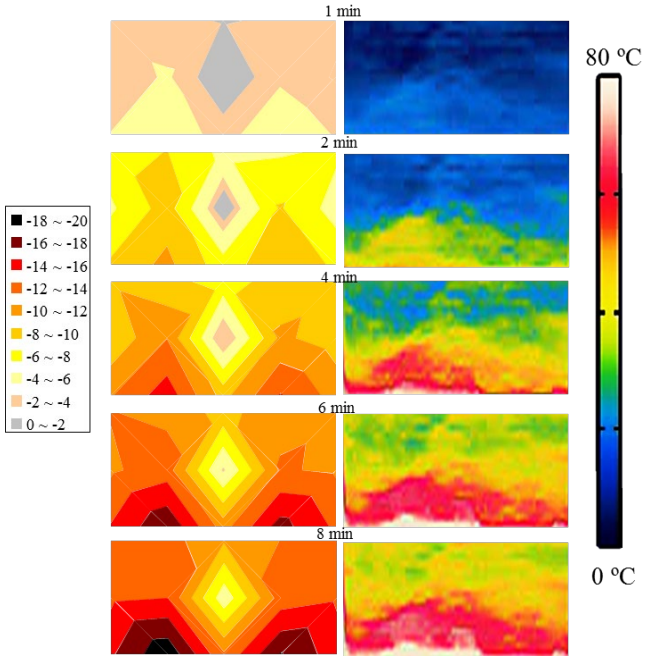


Fig. 8. Detecting thermal conductivity with time using PLDPS (left) and thermogram (right)

3.7 Drilling mapping of PLDPS

Figure 9(a) shows a schematic of an experiment in which a PLDPS is attached to GF/epoxy composites made of e-glass fiber, bisphenol-type epoxy and amine type hardener, and in which a hole is subsequently drilled. This experiment was conducted to evaluate the damage in composites with PLDPS. The paper was coated with pencil lead, and 9 pieces of prove (3 pieces in length and 3 pieces in length with copper wire) were attached using silver paste and epoxy adhesive. The PLDPS was attached to the GF/epoxy composites, and a hole was drilled through the specimen. The ER was compared before and after the hole was drilled, and the damage of GF/epoxy composites was evaluated by 2D mapping methods. Figures 8(b) and (c) show specimen photographs and 2D mapping graphs for specimens of GF epoxy composites with PLDPS attached in which a hole was drilled. The ER of PLDPS changed very rapidly with the specimen impairment and decreased with the distance.

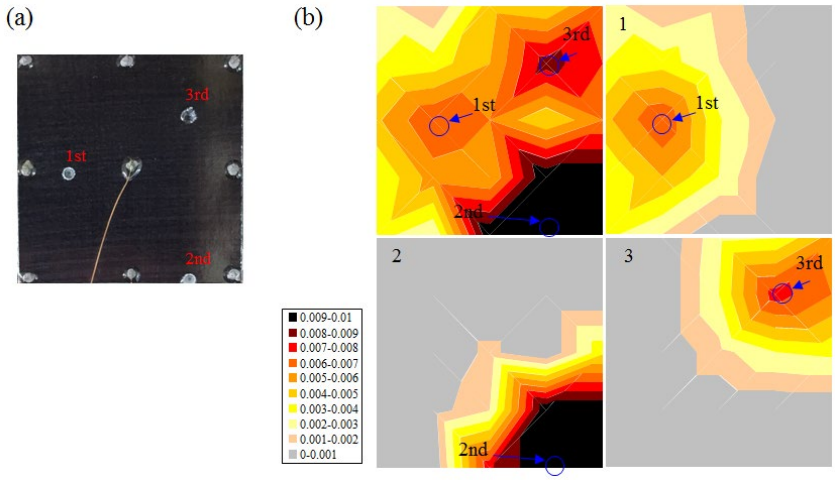


Fig. 9. 2D ER mapping by drilling of holes in GF/epoxy composites: (a) photo of damaged GF/epoxy composites after drilling; and (b) plot of drilling damage detection

4. CONCLUSIONS

Flexible electronic devices have been studied intensively recently and are now being applied to a wide range of fields including human motion robotics. Among them, the devices made by pencil lead and paper are attracting attention because they are inexpensive and can be manufactured quickly. In this work, mechanical properties of PLDPS materials made of pencil lead and paper were evaluated. FT-IR analysis was performed to identify the components of pencil lead and paper, which are the main electrical sensor and a substrate of PLDPS. It was confirmed that the damage was different with the part of the specimen, and the impact, drilling and flexure test were carried out to obtain the results by 2D mapping. The heat transfer of composites was evaluated by thermal mapping using PLDPS as well. The PLDPS, a sensor made of pencil lead and paper, was evaluated and found to have sufficient sensing ability to detect external stimuli such as deformation, damage and heat transfer in materials including composite materials.

5. ACKNOWLEDMENT

This work was supported by the Korea Institute of Energy Technology Evaluation and Planning (KETEP) and the Ministry of Trade, Industry & Energy (MOTIE) of the Republic of Korea (No. 20163030024550).

6. REFERENCES

1. D. J. Kwon, Z. J. Wang, J. J. Kim, K. W. Jang and J. M. Park, Journal of Adhesion and Interface, 14, 75 (2013).
2. Z. J. Wang, D. J. Kwon, G. Y. Gu, J. K. Park, W. I. Lee and J. M. Park, Journal of Adhesion and Interface, 12, 88 (2011).

3. Navratil, R., Kotzianova, A., Halouzka, V., Opletal, T., Triskova, I., Trnkova, L., Hrbac, J., Journal of Electroanalytical Chemistry, vol. 783, 2016, pp. 152–160.
4. Richard, L.M., Chemical Reviews, vol. 108, 2008, pp. 2646–2687.
5. Vytřas, K., Švancara, I., Metelka, R., Journal of the Serbian Chemical Society, vol. 74, 2009, pp. 1021–1033.
6. Christopher, B.J., M., Peairs, J.B., Venton, j., Analytica Chimica Acta, vol. 662, 2010, pp. 105–127.
7. Purushothama, H.T., Nayaka, Y.A, Sensing and Bio-Sensing Research, vol. 16, 2017, pp. 12–18.
8. Gao, W. Song J., Wu N., Journal of Electroanalytical Chemistry, vol. 576, 2005, pp. 1–7.
9. Ng, K,. Gao, B., Yong, K.W., Li, Y., Shi, M., Zhao, X., Li, Z., Zhang, X., Pingguan-Murphy, B., Yang, H., Xu, F., Materials Today, vol. 20, 2017, pp. 32-44.
10. Li, W., Qian, F., Li, Y., Bao, N., Gu, H., Yu, C., Journal of Electroanalytical Chemistry, vol. 769 , 2016, pp. 72–79.